Journal of Hydrology 509 (2014) 282–294

Contents lists available at ScienceDirect

Journal of Hydrology

journal homepage: www.elsevier.com/locate/jhydrol

Linear diffusion-wave channel routing using a discrete Hayami convolution method

Li Wang[a,*], Joan Q. Wu[a], William J. Elliot[b], Fritz R. Fiedler[c], Sergey Lapin[d]

[a] Washington State University, Department of Biological Systems Engineering, Puyallup Research and Extension Center, Puyallup, WA 98371, USA.
[b] US Department of Agriculture, Forest Service, Rocky Mountain Research Station, Moscow, ID 83843, USA
[c] University of Idaho, Department of Civil Engineering, Moscow, ID 83844, USA
[d] Washington State University, Department of Mathematics, Pullman, WA 99164, USA

ARTICLE INFO

Article history:
Received 19 February 2013
Received in revised form 21 October 2013
Accepted 23 November 2013
Available online 1 December 2013
This manuscript was handled by Konstantine P. Georgakakos, Editor-in-Chief, with the assistance of Baxter E. Vieux, Associate Editor

Keywords:
Linear diffusion-wave channel routing
Discrete Hayami convolution
Kernel function values
Mass-balance error
Temporal resolution
Lateral inflow

SUMMARY

The convolution of an input with a response function has been widely used in hydrology as a means to solve various problems analytically. Due to the high computation demand in solving the functions using numerical integration, it is often advantageous to use the discrete convolution instead of the integration of the continuous functions. This approach greatly reduces the amount of the computational work; however, it increases the possibility for mass balance errors. In this study, we analyzed the characteristics of the kernel function for the Hayami convolution solution to the linear diffusion-wave channel routing with distributed lateral inflow. We propose two ways of selection of the discrete kernel function values: using the exact point values or using the center-averaged values. Through a hypothetical example and the applications to Asotin Creek, WA and the Clearwater River, ID, we showed that when the point kernel function values were used in the discrete Hayami convolution (DHC) solution, the mass balance error of channel routing is dependent on the number of time steps on the rising limb of the Hayami kernel function. The mass balance error is negligible when there are more than 1.8 time steps on the rising limb of the kernel function. The fewer time steps on the rising limb, the greater risk of high mass balance errors. When the average kernel function values are used for the DHC solution, however, the mass balance is always maintained, since the integration of the discrete kernel function is always unity.

1. Introduction

In a stream network, the discharge from a given reach depends on the upstream inflow, the storage within the reach, and any gains from, or losses to, lateral flow. Storage is dependent on the micro topography of the valley along the reach. Lateral flow may originate from the interflow through shallow surface layers (Watson and Burnett, 1995), e.g., in steep forests (Dun et al., 2009), or through surface and groundwater interactions. Whether the lateral flow is positive or negative will depend on the relative hydraulic gradient between the channel stage and the adjacent water table.

Open-channel flow is typically simplified as one-dimensional flow processes described by the Saint–Venant equations, which consist of the continuity equation and the momentum equation (Chow et al., 1988; Singh et al., 1997). There are three methods based on the simplifications to the momentum equation: the dynamic-wave method that considers all the terms in the momentum equation, the diffusion-wave method that neglects the acceleration terms, and the kinematic-wave method that neglects both the acceleration and pressure force terms (Chow et al., 1988; Singh et al., 1997). Among these three methods, the diffusion-wave method is widely used because it is easier to implement compared to the dynamic-wave method, yet still gives sufficiently accurate results (Moussa, 1996; Moussa and Bocquillon, 1996; Singh et al., 1997; Wang et al., 2003; Fan and Li, 2006; Moramarco et al., 2008).

Combined with the Manning's equation or the Chezy's equation, the diffusion-wave equations can be simplified to one single equation (Moussa, 1996; Fan and Li, 2006). With the assumption of constant wave celerity and diffusion coefficient, this equation has been solved analytically to give the convolution solution (Hayami, 1951; Ogata and Banks, 1961; Moussa, 1996; Fan and Li, 2006). For simplified diffusion-wave channel routing without lateral inflow,

Abbreviations: AKF, average kernel function; CPMC, constant-parameter Muskingum–Cunge; DHC, discrete Hayami convolution method; DHC-AKF, discrete Hayami convolution solution with average kernel function values; DHC-PKF, discrete Hayami convolution solution with point kernel function values; PKF, point kernel function; RMSE, root-mean-square error; USDA, United States Department of Agriculture; USGS, United States Geological Survey; WADOE, Washington State Department of Ecology.

* Corresponding author. Present address: GeoEngineers, Inc., Tacoma, WA 98402, USA. Tel.: +1 253 445 4565; fax: +1 253 445 4621.
E-mail address: liwang@wsu.edu (L. Wang).

0022-1694/$ - see front matter © 2013 Elsevier B.V. All rights reserved.
http://dx.doi.org/10.1016/j.jhydrol.2013.11.046

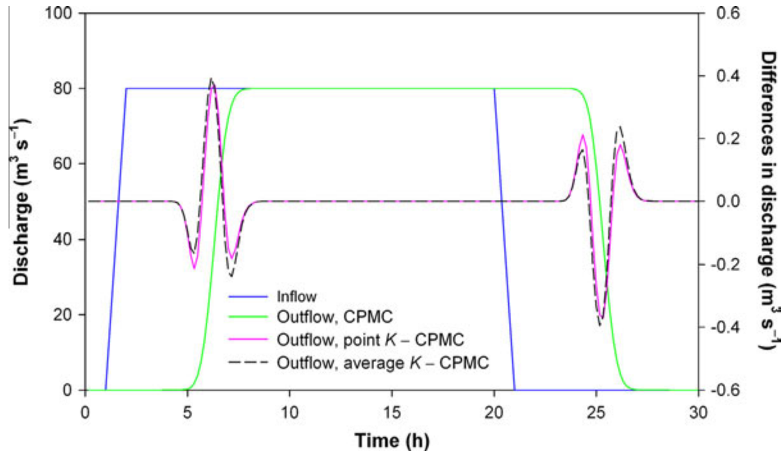

Fig. 1. Comparison of discrete convolution method and the constant-parameter Muskingum–Cunge (CPMC) method for a time step of 600 s. Note that simulated outflows from the discrete Hayami solution and the CPMC method largely overlap, and therefore only the differences between the two methods are shown.

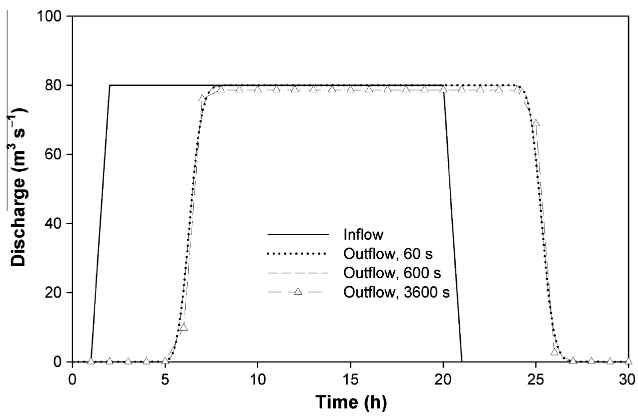

Fig. 2. Discrete Hayami convolution solutions using point kernel function values for different sizes of time step. The solutions for 600-s and 60-s time steps largely overlap. For the time step of 3600 s, the calculated peak discharge is 1.7% lower than the theoretical value.

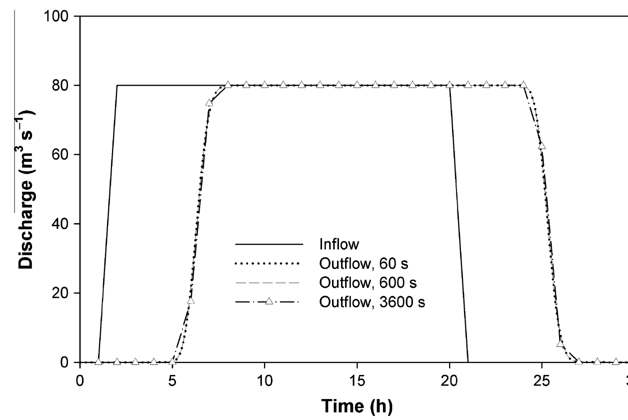

Fig. 4. Discrete Hayami convolution solution using average kernel function values. The calculated peak discharge is not affected by the size of time step. The solutions for the 60-s and 600-s time steps largely overlap, and the calculated peak discharge is the same for all three time steps.

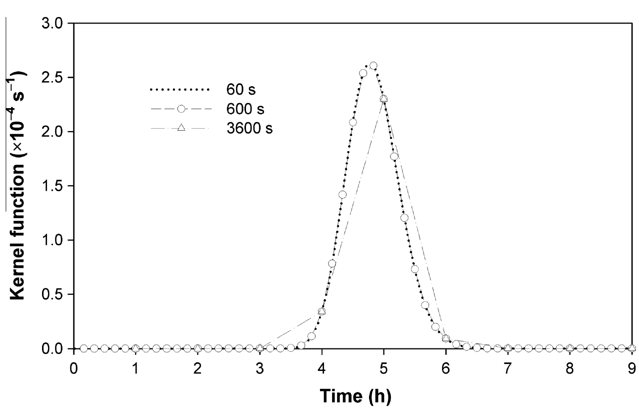

Fig. 3. Discrete Hayami kernel functions with point values for different sizes of time step.

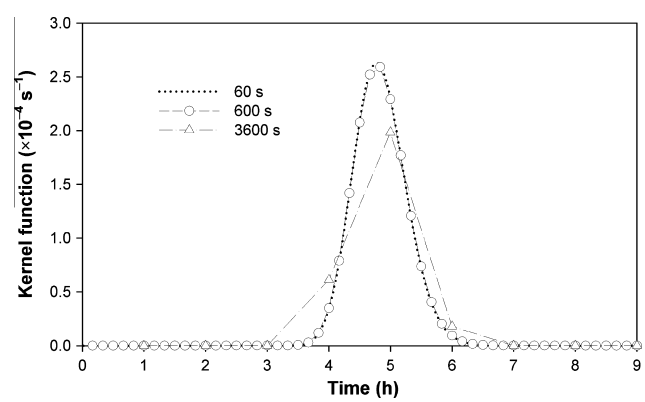

Fig. 5. Discrete Hayami kernel function from using average values for different sizes of time step.

we can obtain the analytical convolution equation and solve it analytically or by numerical integration techniques. Assuming no lateral inflow, Hayami (1951) solved the linear diffusion-wave model using perturbation theory, and obtained the analytical solution in terms of water depth in convolution form. He also found that, for the linear diffusion wave, the unit-graph method could be used to approximate the analytical solution for appropriate time step sizes. Tingsanchali and Manandhar (1985) developed the convolution solution for diffusion-wave channel routing considering lateral inflow and backwater effect. Through a Laplace transform, Moussa (1996) obtained the convolution solution for the linear diffusion-wave model taking into consideration of distributed lateral inflow with a steady-state initial condition. Fan and Li

(2006) further extended the solution for linear diffusion-wave channel routing with distributed or concentrated lateral inflow, and analyzed outflow change as affected by different boundary conditions.

The method of convolving an input with a kernel function has been applied to various arenas in hydrology to obtain the analytical solution of the output. Dooge (1959) convoluted rainfall data with the instantaneous unit hydrograph to calculate the rainfall response at an outlet of a channel or watershed. Barlow et al. (2000) and Hantush (2005) applied the convolution solution to one-dimensional surface water-groundwater interactions, considering the effects of channel inflow, lateral inflow, groundwater recharge, and hydraulic gradients between surface and groundwater. Olsthoorn (2008) presented case applications of the convolution method to analysis of fluctuations of groundwater level as affected by local and remote recharges, and drawdown calculation of pumping tests. McGuire et al. (2005) applied the convolution method to examining tracer movement to estimate water residence times within a watershed. Ogata and Banks (1961) solved the diffusion-wave equation (in the same form as for channel flow) for mass transport in groundwater flow, and obtained the convolution solution.

The major advantages of the analytical solutions over numerical methods in channel-flow routing are that the former are usually unconditionally stable and computationally more efficient (Hayami, 1951; Chaudhry, 1993, p. 370; Moussa, 1996; Fan and Li, 2006). However, analytical solutions can only be obtained for limited, special cases. For a simplified case with a constant inflow at the upper boundary and homogenous initial condition, Ogata and Banks (1961) found that the convolution solution can be expressed in terms of error functions, which have tabulated values and can be

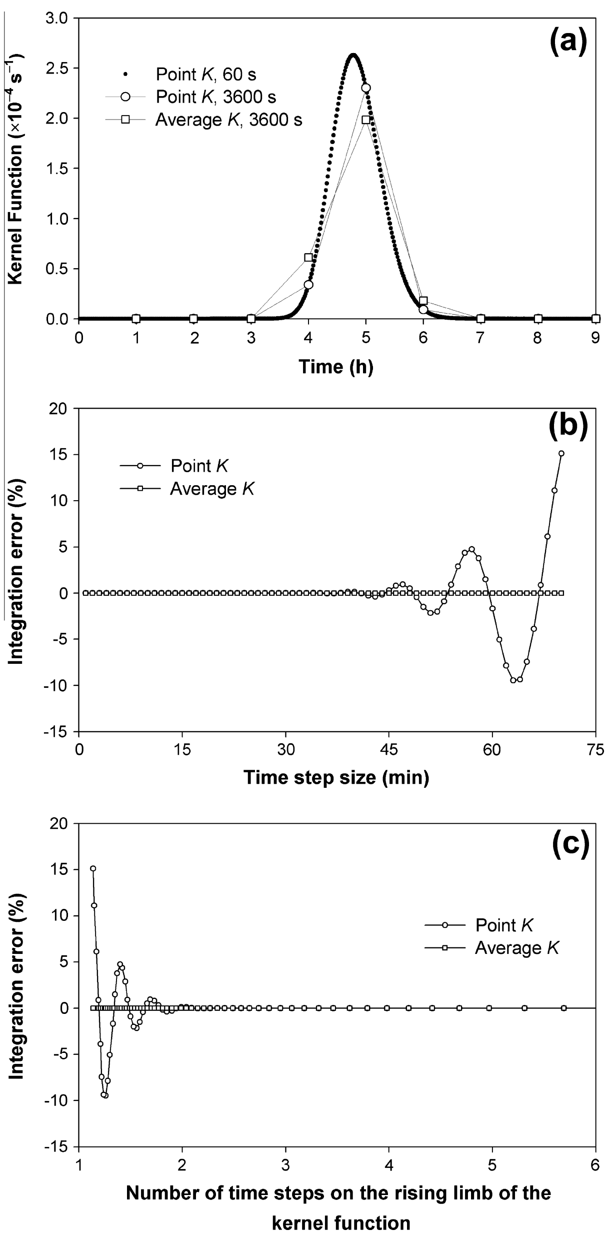

Fig. 6. Comparison of discrete Hayami kernel functions using point- or average values (a), and the effect of the size of time step (b) and the number of time steps (c) on the integration error.

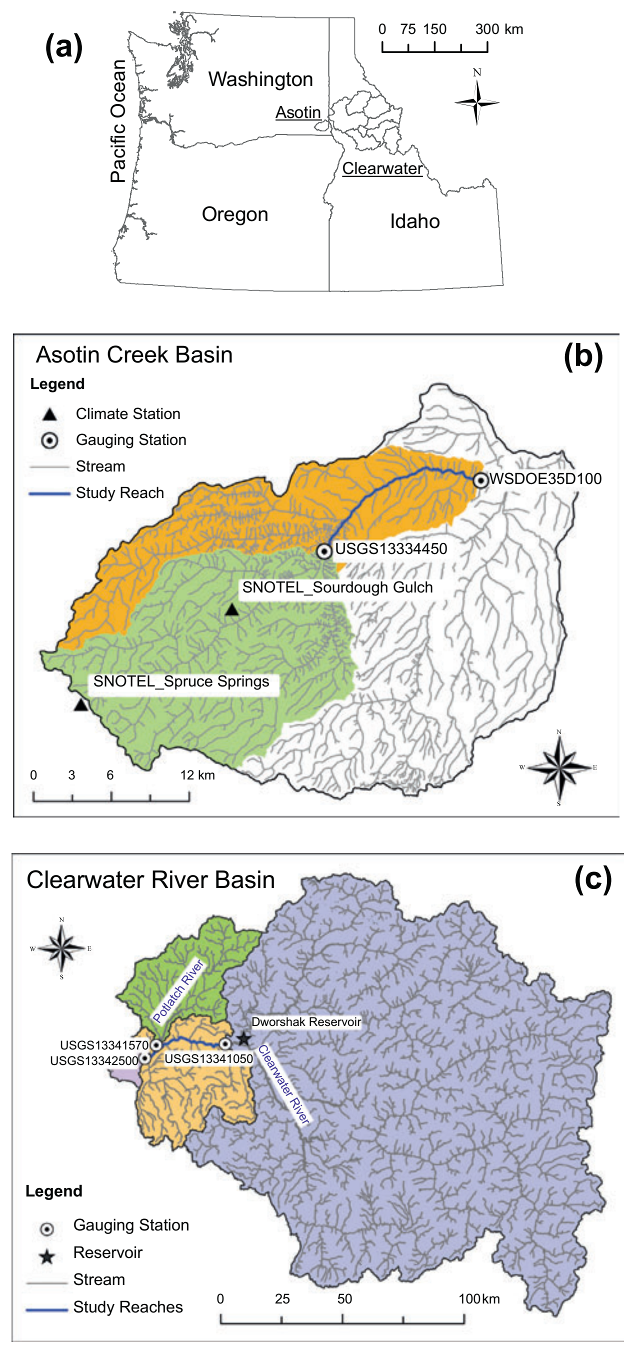

Fig. 7. (a) Location of Asotin Creek and Clearwater River basins, northwestern US, (b) Asotin Creek basin, and (c) Clearwater River basin.

readily solved using computer programs. When the lateral inflow is a significant component of the channel inflow, the wave celerity and diffusion coefficient can no longer be considered constant for the entire channel reach. Moussa and Bocquillon (1996) suggested the use of numerical methods in such cases. In general, we need to solve the convolution equations by numerical integration, which is time-consuming and limits the applications of the analytical solution (Munier et al., 2008). To obtain the analytical solution efficiently when the inflows are at a constant temporal interval, we can apply discrete methods to approximate the continuous convolution solution (Chow et al., 1988, p. 204; Long, 2009) or use the simplified transfer function approach which ensures the mass balance closure and takes into account the acceleration terms and the backwater effects (Munier et al., 2008).

In a discrete method, the input is given as a series of data values at a specified temporal interval, and the solution is obtained at the same temporal coordinates as the input. Discrete methods have been widely used in hydrology, such as in the unit hydrograph method (Dooge, 1959; Chow et al., 1988), the discrete cascade models based on the Muskingum reservoir method (O'Connor, 1976; Perumal, 1994; Camacho and Lees, 1999; Perumal et al., 2007), the discrete convolution methods for estimating surface water–groundwater interactions (Barlow et al., 2000; Hantush et al., 2002; Hantush, 2005), and the discrete convolution method for diffusion-wave channel routing (Tingsanchali and Manandhar, 1985).

In all aforementioned discrete methods, the response function should sum to unity for mass balance. Chow et al. (1988, p. 218) suggested to scale up or down the corresponding response function values if their summation does not meet this criterion. This remedy is easy to implement but it may shift the kernel function curve. Hence, this approach is not recommended when the accuracy of peak time is important for a specific study. The cause of the mass-balance error is due to the coarse temporal resolution. In order to achieve more accurate results of the discrete convolution solution, Barlow et al. (2000) proposed to use smaller time steps. In most applications, the time step in the observation data is fixed, and it would be important to know whether the given temporal interval is sufficiently fine. It may be feasible to determine the adequate time-step size with an acceptable mass-balance error by comparing simulation results from different time-step sizes for small watersheds with a few channel reaches. However, in large watershed modeling there may be hundreds or thousands of channel reaches. The computing cost for determining an appropriate time step could become very high.

The objective of this study was to investigate the characteristics of the Hayami kernel function to (i) develop criteria for adequate temporal resolutions, and (ii) identify the appropriate discrete Hayami method for accurate channel routing. Based on the channel-flow solution by Moussa (1996), we analyzed the Hayami kernel function and demonstrated our analysis in a numerical experiment and applied it to two streams in Northwestern USA. The major sections include: Introduction, Diffusion-wave model with lateral inflow, A numerical experiment, Applications, and Summary and Conclusions.

2. Diffusion-wave model with lateral inflow

2.1. General solution

When the friction slope of the water surface is much smaller than the channel bed slope, the linear convection–diffusion

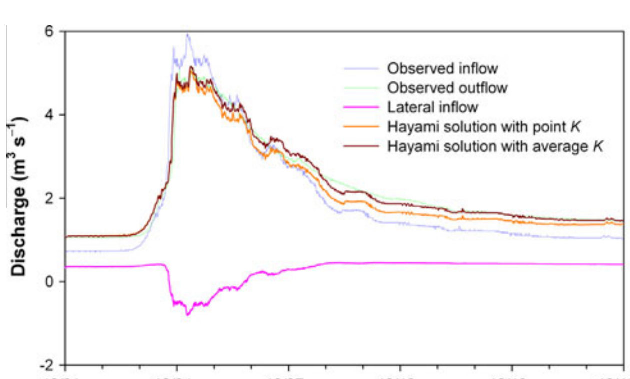

Fig. 8. Observed and simulated hydrographs for Asotin Creek, WA, in response to the rainfall and snowmelt events during December 1–16, 2007.

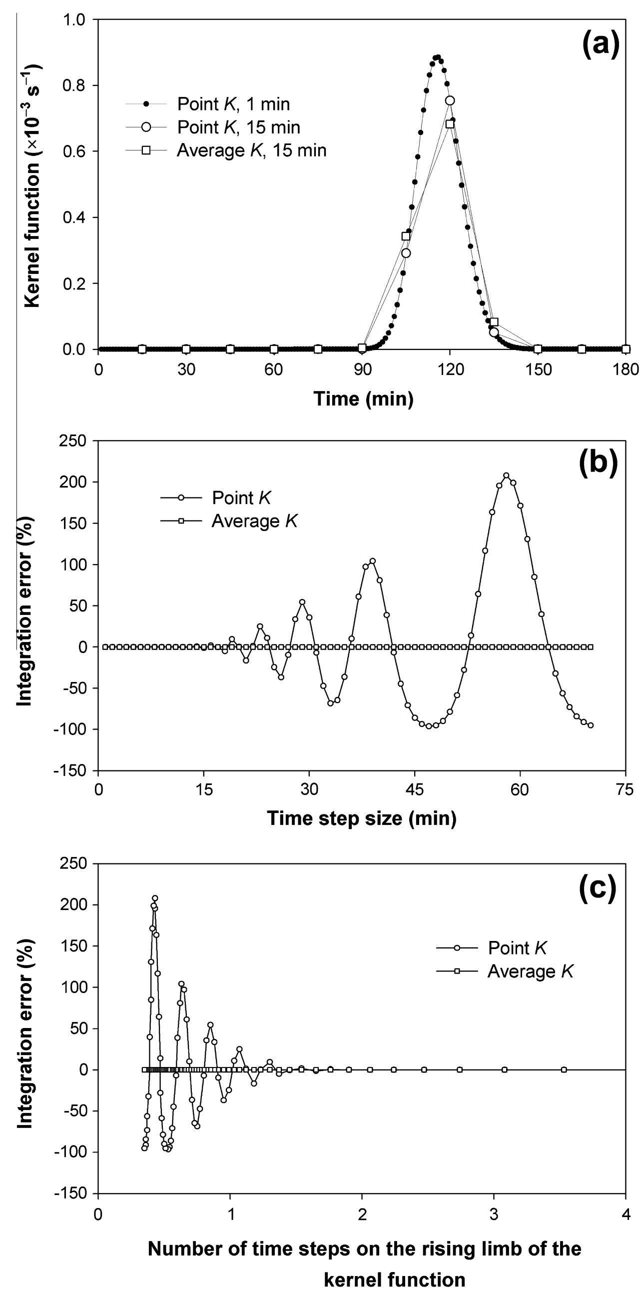

Fig. 9. Comparison of discrete Hayami kernel functions using point- or average values (a), and the effect of the size of time step (b) and the number of time steps (c) on the integration error in the discrete Hayami kernel function for channel flow routing, Asotin Creek, WA, December 1–16, 2007.

equation with uniformly distributed lateral inflow can be simplified as (Lighthill and Whitham, 1955; Moussa, 1996; Fan and Li, 2006)

$$\frac{\partial Q}{\partial t} + C\frac{\partial Q}{\partial x} - D\frac{\partial^2 Q}{\partial x^2} = Cq \tag{1}$$

where x is the downstream distance (m), t, time (s), Q, discharge ($m^3\,s^{-1}$), q, lateral inflow rate per unit length ($m^2\,s^{-1}$), $C = \frac{dQ}{dA}$, wave celerity ($m\,s^{-1}$), $D = \frac{Q}{2BS_f} \approx \frac{Q}{2BS_0}$, diffusive coefficient ($m^2\,s^{-1}$), A, cross-sectional area (m^2), B, channel width at the water surface (m), S_f, friction slope, and S_0, channel bed slope. The calculations of C and D are dependent on the type of the channel cross section and the selection of the reference discharge (Chow et al., 1988; Ponce and Chaganti, 1994).

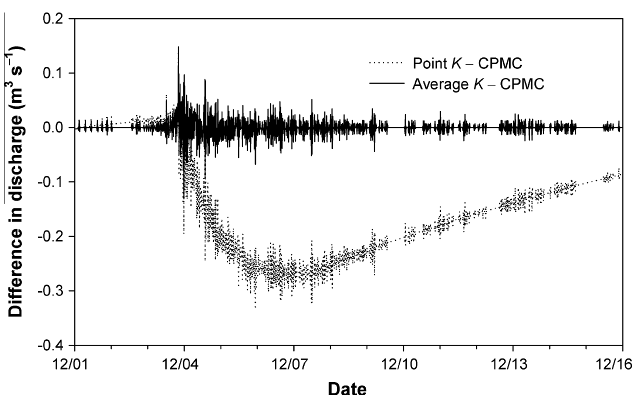

Fig. 10. Differences in simulated discharges between the Hayami discrete convolution methods with point- or average kernel function values and the constant-parameter Muskingum–Cunge (CPMC) method, Asotin Creek, WA, December 1–16, 2007.

For channel flow with steady-state initial conditions, the Hayami solution is (Moussa, 1996)

$$Q(x,t) = Q(x,0) + \Phi(t) + [Q(0,t) - Q(0,0) - \Phi(t)] \otimes K(t) \tag{2}$$

where $\otimes$ is the convolution sign, and $K(t)$ is the Hayami kernel function defined as

$$K(t) = \frac{x}{2\sqrt{\pi D t^3}} e^{-\frac{(x-Ct)^2}{4Dt}} \tag{3}$$

and $\Phi(t)$ is a term related to the wave celerity and the lateral inflow

$$\Phi(t) = C\int_0^t [q(\tau) - q(0)]d\tau \tag{4}$$

2.2. Discrete Hayami convolution solution with exact point kernel function values (DHC-PKF)

2.2.1. Expression of the exact point kernel function

When the channel inflow at the upper boundary is in a discrete form, Eq. (2) for the outlet can be written as

$$Q^n = Q^0 + \Phi^n + \Delta t\sum_{j=0}^{n-1}\left[Q_u^j - Q_u^0 - \Phi^j\right]K^{n-j} \tag{5}$$

where Δt is the time step, n is the numbers of time steps, Q^n and Q^0 are the channel flow rate at the outlet at time $t^n = n\Delta t$ and time 0, respectively, Φ^n and Φ^j are the discrete form of $\Phi(t)$ at time $n\Delta t$ and $j\Delta t$, respectively, Q_u^j and Q_u^0 are the channel inflow at the upper boundary at time $j\Delta t$ and 0, respectively, and, K^j is the discrete kernel function value at time step j

$$K^j = \frac{x}{2\sqrt{\pi D (j\Delta t)^3}} e^{-\frac{(x-Cj\Delta t)^2}{4Dj\Delta t}}, \quad j = 1, 2, 3, \ldots \tag{6}$$

The term K^0 is omitted because its value is always zero.

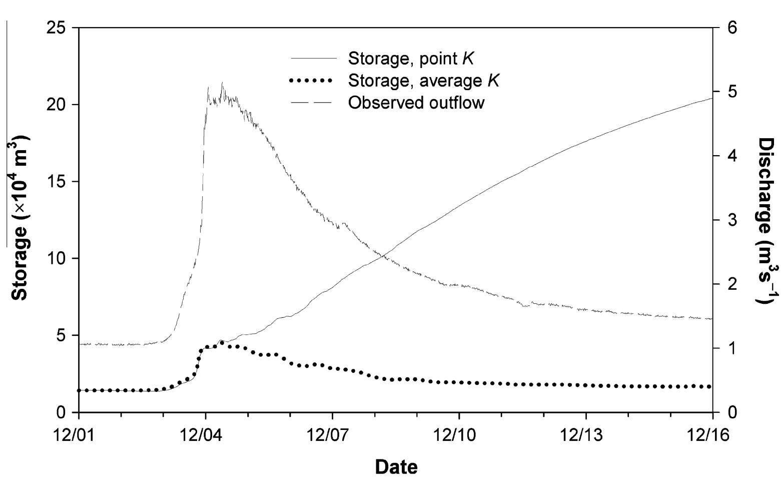

Fig. 11. Simulated channel water storage by different methods, Asotin Creek, WA, December 1–16, 2007. Note that the simulated storages using the discrete Hayami solution with average kernel function values and using the constant-parameter Muskingum–Cunge method largely overlap, thus only the former is shown.

Table 1
USGS gauging stations on Clearwater River near Peck and Spalding, ID.

USGS station	River	Location	River mile (River km)	Drainage Area mi² (km²)	Elevation (m)
13341050[a]	Clearwater	Near Peck, ID	37.4 (60.2)	7976 (20,660)	930
13342500[b]	Clearwater	At Spalding, ID	11.6 (18.7)	9283 (24,040)	770
13341570	Potlatch	Below Little Potlatch Cr. near Spalding, ID	2.0 (3.2)	583 (1510)	845

[a] Inflow station.
[b] Outflow station.

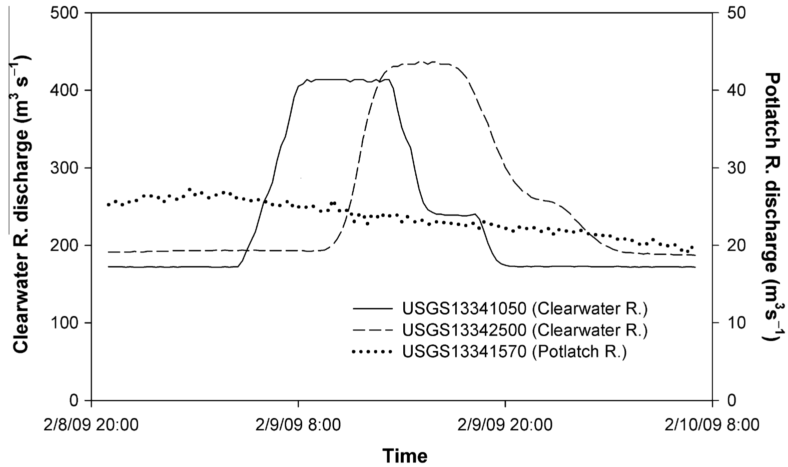

Fig. 12. Observed hydrographs at the three gauging stations on Clearwater River and its tributary Potlatch River. Note different discharge scales used.

Eq. (5) is the DHC-PKF values K^j ($j = 1,2,3,\ldots$). The accuracy of the discrete convolution results depends on the time step size Δt and can be improved by decreasing Δt (Barlow et al., 2000). As the original kernel function is continuous and its integration is 1, the summation of its discrete form should also be unity for otherwise mass balance would not be maintained. However, when the time step becomes too large, there may be only a few discrete points left on the rising curve of the kernel function, causing the discrete integration of K^j to be larger or smaller than unity and thus an error in mass balance. Knowing the expression of the discrete kernel function, it is possible to define a maximum time step that ensures sufficient accuracy.

2.2.2. Determination of maximum time step

To determine a maximum time step, we first calculate the maximum K value, and estimate the time for K to rise from a small value, e.g., 0.1% of the maximum, to the maximum value.

From Eq. (3), we have

$$K'(t) = -\frac{3}{2}\frac{x}{2\sqrt{\pi D t^5}}e^{-\frac{(x-Ct)^2}{4Dt}} + \frac{x}{2\sqrt{\pi D t^3}}e^{-\frac{(x-Ct)^2}{4Dt}}\left[\frac{C(x-Ct)}{2Dt} + \frac{(x-Ct)^2}{4Dt^2}\right]$$
$$= \frac{x}{2\sqrt{\pi D t^5}}\left(-\frac{3}{2} + \frac{x^2 - C^2t^2}{4Dt}\right)e^{-\frac{(x-Ct)^2}{4Dt}} \quad (7)$$

Letting $K'(t) = 0$, and neglecting the negative solution, we obtain

$$t_{km} = \frac{3D}{C^2}\left[\sqrt{1 + \left(\frac{Cx}{3D}\right)^2} - 1\right] \quad (8)$$

where t_{km} is the time when K reaches its maximum value $K_{\max}$.

If the dynamics is dominated by diffusion ($Cx \ll D$, or $P_e = \frac{Cx}{2D} \ll 1$), $t_{km} = \frac{x^2}{6D}$, whereas if convection dominates ($P_e \gg 1$), $t_{km} = \frac{x}{C}$.

Letting $K(t) = 0.001K_{\max}$ and using Newton's method, we can obtain t_l, the time when K reaches 0.1% of $K_{\max}$ on the rising limb. The maximum time step for channel routing using Eq. (5) can then be estimated as

$$\Delta t_{\max} = \frac{t_{km} - t_l}{N} \quad (9)$$

where N is the number of time steps on the rising limb and can be varied to attain the desired resolution.

Higdon (2002) obtained satisfactory results with a discrete spatial interval close to the standard deviation of the Gaussian kernel function ($N \geqslant 3$). The principle of discrete convolution in a space

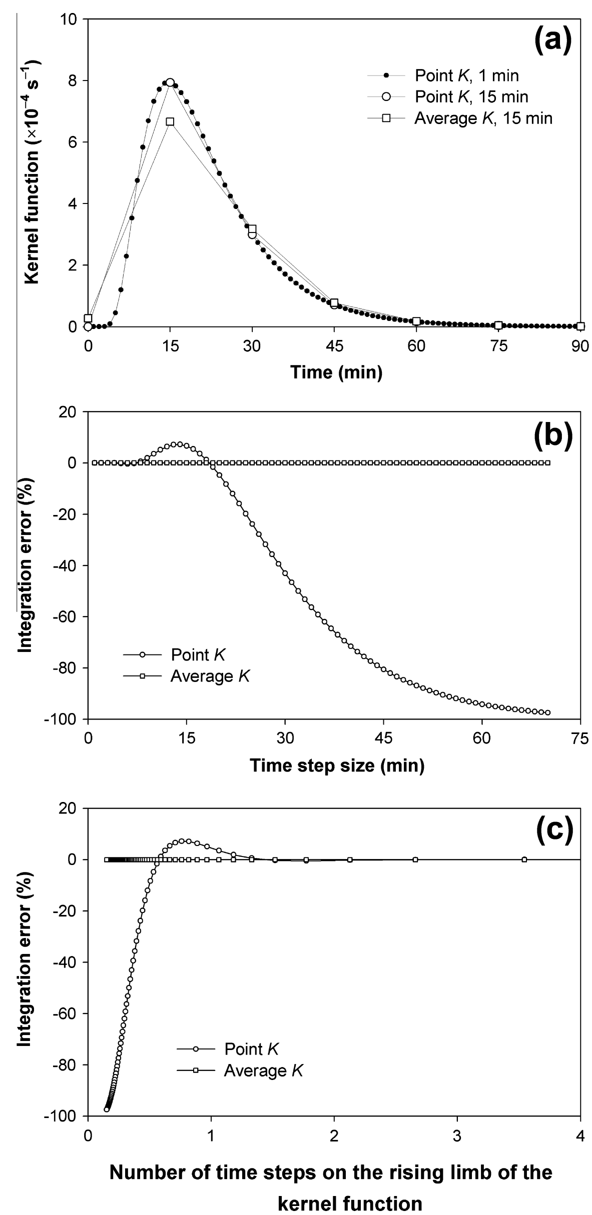

Fig. 13. Comparison of discrete Hayami kernel functions using point- or average values (a), and the effect of the size of time step (b) and the number of time steps (c) on the integration error in the discrete Hayami kernel function for channel flow routing, Potlatch River, ID, February 8–10, 2009.

domain is the same as in a time domain. For a greater accuracy, Merkel (2002) suggested the use of 10 time steps to assure an adequate resolution of the rising limb of a hydrograph.

2.3. Discrete Hayami convolution solution with average kernel function values (DHC-AKF)

In the unit-step response method, the average of K^j is calculated from time t to $t+\Delta t$ (Dooge, 1959; Chow et al., 1988, p. 207; Hantush et al., 2002; Hantush, 2005). As a replacement of the exact point kernel function value K^j, the center average of K^j around a discrete point j can be calculated using the following equation

$$\begin{aligned}\overline{K}^j &= \frac{1}{\Delta t}\int_{t^{j-1/2}}^{t^{j+1/2}} K(\tau)\mathrm{d}\tau \\ &= \frac{1}{\Delta t}\left[\int_0^{t^{j+1/2}} K(\tau)\mathrm{d}\tau - \int_0^{t^{j-1/2}} K(\tau)\mathrm{d}\tau\right] \quad \text{for } j = 1,2,\ldots,n \\ &= \frac{1}{\Delta t}\left[S(t^{j+1/2}) - S(t^{j-1/2})\right]\end{aligned}$$

and

$$\overline{K}^0 = \frac{2}{\Delta t}S(t^{1/2}) \qquad \text{for } j = 0 \tag{10}$$

where j is the time step number, t^j is the time (s) at step j, and $S(t)$ is the storage function (Dooge, 1959; Fan and Li, 2006), which is the same as the unit-step response function (Chow et al., 1988, p. 205) and is given by (Ogata and Banks, 1961; Fan and Li, 2006)

$$S(t) = \int_0^t K(\tau)\mathrm{d}\tau = \frac{1}{2}\left[erfc\left(\frac{x-Ct}{2\sqrt{Dt}}\right) + e^{\frac{Cx}{D}} erfc\left(\frac{x+Ct}{2\sqrt{Dt}}\right)\right] \tag{11}$$

Substituting $\overline{K}^j$ for K^j in Eq. (5), we have

$$\begin{aligned}Q^n &= Q^0 + \Phi^n + \sum_{j=0}^{n-1}\left(Q_u^j - Q_u^0 - \Phi^j\right)\left[S(t^{n-j+1/2}) - S(t^{n-j-1/2})\right] \\ &\quad + \left(Q_u^n - Q_u^0 - \Phi^n\right)S(t^{1/2})\end{aligned} \tag{12}$$

Eq. (12) is the discrete convolution solution to Eq. (1) using the AKF values $\overline{K}^j$ ($j = 0,1,2,3,\ldots$). Note the difference between the AKF and the PKF at time zero: the value of the former at time zero, $\overline{K}^0$, may not be zero. The use of the AKF preserves mass balance better since the storage function approaches unity for sufficiently large time (Fan and Li, 2006). This can be seen from the integration of the Hayami kernel function as time approaches infinity:

$$\begin{aligned}\lim_{t\to\infty} S(t) &= \lim_{t\to\infty}\left\{\frac{1}{2}\left[erfc\left(\frac{x-Ct}{2\sqrt{Dt}}\right) + e^{\frac{Cx}{D}} erfc\left(\frac{x+Ct}{2\sqrt{Dt}}\right)\right]\right\} \\ &= \lim_{t\to\infty}\left\{\frac{1}{2}\left[2 + e^{\frac{Cx}{D}}\cdot 0\right]\right\} = 1\end{aligned} \tag{13}$$

When the discrete convolution solution is used to calculate the discharge, the time step in the kernel function must be the same as in the input discharge. If the time step is smaller than $\Delta t_{\max}$ in Eq. (9), Eqs. (5) and (6) can be used to calculate channel flow.

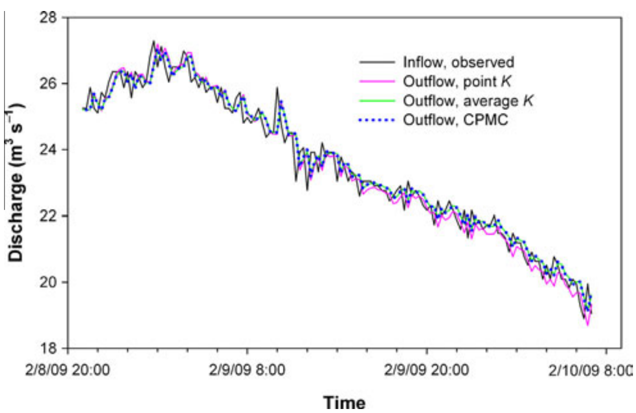

Fig. 14. Observed inflow and simulated outflow for the Potlatch River (with the assumption of no lateral inflow), February 8–10, 2009. The results from the discrete Hayami solution using the average kernel function values and the CPMC method largely overlap.

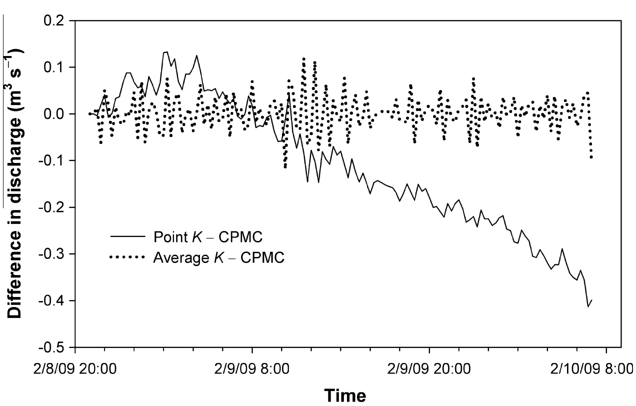

Fig. 15. Differences in discharges between the discrete Hayami convolution solution and the CPMC method, Potlatch River, ID, February 8–10, 2009.

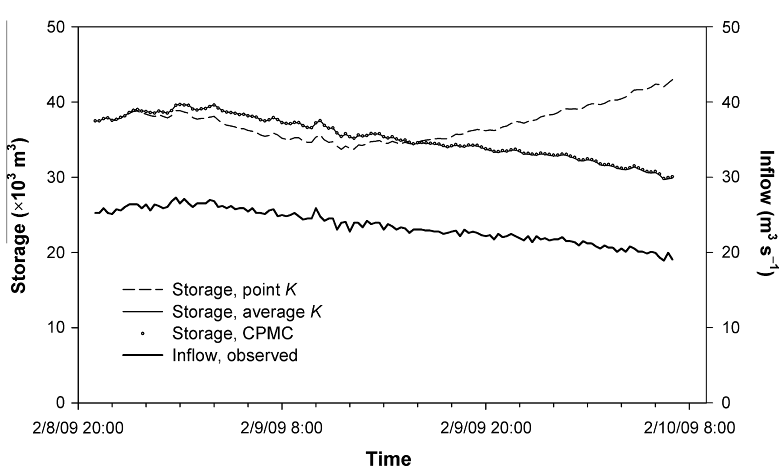

Fig. 16. Simulated channel storage using different methods, Potlatch River, ID, February 8–10, 2009. Note that the simulated storages from the discrete Hayami solution using the average kernel function values and the CPMC method largely overlap.

Otherwise, we either interpolate the known discharges (Merkel, 2002) or use Eqs. (11) and (12) to calculate channel flow, to assure mass balance and adequate accuracy.

2.4. Integration error of the discrete kernel function

For a constant inflow with homogenous initial condition and with no lateral inflow within the stream reach, the relative mass balance error of outflow resulting from the discrete kernel function is the same as the integration error of the discrete kernel function

$$\begin{aligned}\Delta M &= \left(1-\Delta t\sum_{j=1}^{\infty}\frac{K^{j-1}+K^{j}}{2}\right)\times 100\% \\ &= \left[1-\Delta t\left(\sum_{j=1}^{\infty}\frac{K^{j-1}}{2}+\sum_{j=1}^{\infty}\frac{K^{j}}{2}\right)\right]\times 100\% \\ &= \left[1-\Delta t\left(\frac{K^{0}}{2}+\sum_{j=1}^{\infty}\frac{K^{j}}{2}+\sum_{j=1}^{\infty}\frac{K^{j}}{2}\right)\right]\times 100\% \\ &= \left[1-\Delta t\left(\frac{K^{0}}{2}+\sum_{j=1}^{\infty}K^{j}\right)\right]\times 100\% \qquad (14)\end{aligned}$$

For channel routing with lateral inflow or when channel inflow at the upper boundary varies with time, the total mass balance error for the simulated outflow will be $\Delta M \times \Delta t\sum_{j=0}^{n-1}\left(Q_u^j - Q_u^0 - \Phi^j\right)$.

2.5. Channel water storage

To track the channel water balance, we first calculate the initial cross-section area for the steady-state channel inflow and outflow using Manning's equation, and estimate the initial channel water storage (S^0, m^3) by multiplying the average cross-section area by the channel length. The storage S^j (m^3) at time t^j is calculated by (Todini, 2007)

$$\begin{aligned}S^j &= S^{j-1} + V_{in} - V_{out} \\ &= S^{j-1} + \left(\frac{Q_u^j + Q_u^{j-1}}{2} + \frac{q^j + q^{j-1}}{2}x\right)\Delta t - \left(\frac{Q^j + Q^{j-1}}{2}\right)\Delta t,\\ j &= 1,2,3,\ldots \qquad (15)\end{aligned}$$

3. A numerical experiment

For a numerical experiment, we assume a rectangular channel with width $B = 50$ m, length $L = 30{,}000$ m, Manning's roughness $n = 0.035$, bed slope $S_0 = 0.002$, and the following initial and boundary conditions

At $t = 0$,

$$Q(x,0) = 0, \quad x \geqslant 0 \qquad (16)$$

At $x = 0$,

$$\left.\begin{array}{ll} Q(0,t) = 0, & 0 < t < 3600 \\ Q(0,t) = 80 \times \frac{t-3600}{3600}, & 3600 \leqslant t < 7200 \\ Q(0,t) = 80, & 7200 \leqslant t \leqslant 72{,}000 \\ Q(0,t) = 80 \times \frac{75{,}600-t}{3600}, & 72{,}000 < t < 75{,}600 \\ Q(0,t) = 0, & 75{,}600 \leqslant t \end{array}\right\} \qquad (17)$$

where t is in s, x in m, and Q in $m^3\,s^{-1}$.

With the assumed channel characterization and discharge, the wave celerity C can be estimated by $C = \left(1 + \frac{2B}{3(B+2y)}\right)\frac{Q}{By}$, in which y is the depth of water and can be calculated from Manning's equation using Newton's method (Chow et al., 1988). The calculated C is 2.25 m s^{-1}, and the diffusive coefficient D is 400 $m^2\,s^{-1}$.

3.1. Comparison of discrete convolution solutions with Muskingum–Cunge solution

Fig. 1 shows the results from the discrete convolution solutions and the constant-parameter Muskingum–Cunge (CPMC) method (Ponce and Chaganti, 1994) for a time step of 600 s. Both discrete convolution solutions, with PKF or AKF values, compare well with

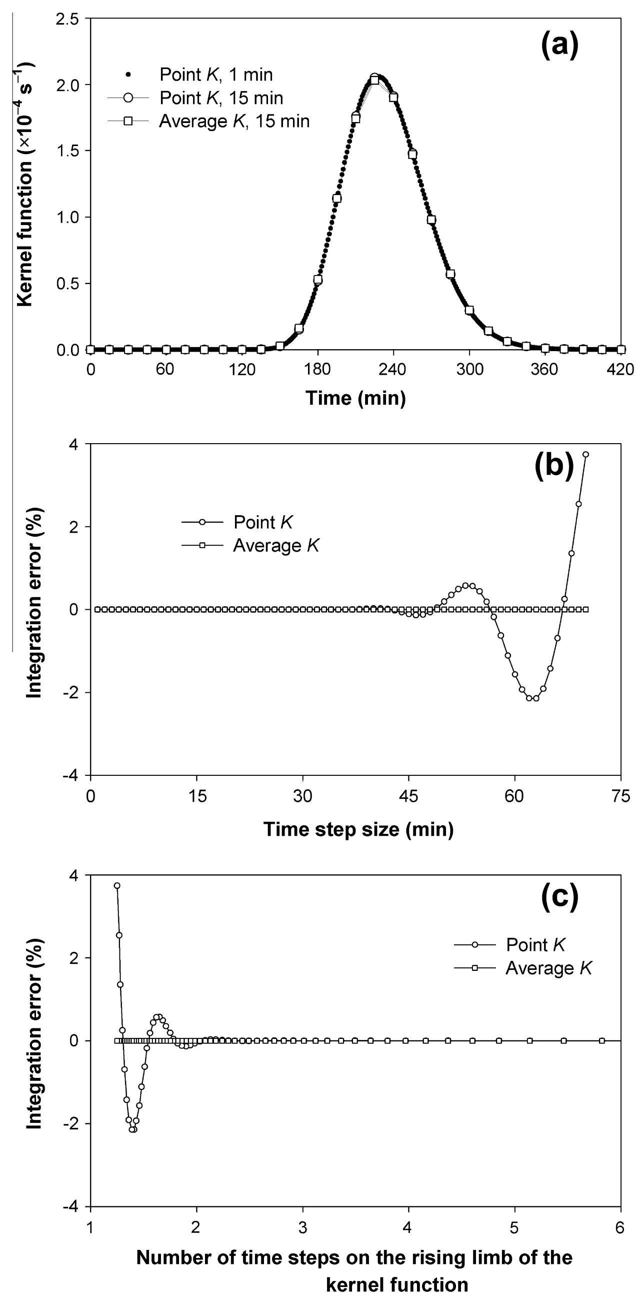

Fig. 17. Comparison of discrete Hayami kernel functions with point- or average values (a), and the effect of the size of time step (b) and the number of time steps (c) on the integration error in the discrete Hayami kernel function for channel flow routing, upper reach, Clearwater River, ID, February 8–10, 2009.

the CPMC solution. The differences (maximum 0.5%) occur only along the rising and falling limbs (Fig. 1).

3.2. Discrete convolution solution with PKF and AKF values

When the time step is small, the DHC-PKF method gives satisfactory results (Fig. 2). For the hypothetical case described by Eqs. (16) and (17), the difference between the results with a time step of 600 s or 60 s is negligible. The respective N values are 8 and 80, with the rising limb of the kernel function starting at $t = 12{,}425$ s and reaching the maximum at $t = 17{,}200$ s (Fig. 3). For the time step of 3600 s, however, the calculated peak discharge is 78.7 $m^3 s^{-1}$, 1.7% lower than the theoretical value of 80.0 $m^3 s^{-1}$. This error is caused by the inadequate resolution of the discrete kernel function. When the time step is increased to 3600 s, $N = 1.33$, and the integration of the discrete Hayami kernel function is not unity (Fig. 3), resulting in the mass balance error.

The use of AKF values always preserves mass balance. The simulated peak discharge is the same for different sizes of time steps (Fig. 4) and the integration of the discrete kernel function is always unity (Fig. 5).

3.3. Comparison of different calculation methods for discrete kernel function and temporal resolution

For the relatively small time step of 60 s, the calculated discrete kernel functions using the point- or average values are almost the same. For the time step of 3600 s, the two calculation methods lead to different results (Fig. 6a). The point K values do not coincide with the average K values, indicating their failure to represent the average K values of the analytical solution within the corresponding time step. The discrete integration of the PKF is not unity, resulting in mass balance error.

When the discrete Hayami kernel function with average values is used, the integration error of the kernel function in calculated outflow is independent of the size of time step (Fig. 6b and c). This is because the storage function always reaches unity given sufficiently long time. When the discrete kernel function with point values is used, the temporal resolution will affect the integration of the kernel function, and hence the accuracy of mass balance. The relative integration error ΔM ranges from −9.4% to 15% for 1.14–1.73 time steps on the rising limb, and is less than 0.38% when the rising limb is longer than 1.77 time steps or for $\Delta t < 45$ min (Fig. 6b and c).

3.4. Computing cost

On a Pentium 4 PC, the CPU time for running the FORTRAN program with the DHC-PKF or the DHC-AKF method is 0.125 s for 2000 time steps, the same as for running the CPMC solution.

4. Applications

We chose two streams in the Northwestern USA for our application, the Asotin Creek, WA, and the Clearwater River, ID (Fig. 7).

4.1. Asotin Creek, WA

Asotin Creek is located in eastern Washington State, USA (Fig. 7a). It joins the Snake River at Asotin, WA. The watershed is typical of many watersheds in the western USA, with high-elevation snowmelt providing much of the runoff. Streamside agriculture and domestic users are dependent on the streamflow for livestock, irrigation, and human consumption. Much of the development has been, and continues to be, in the flood plains. Therefore, understanding fluctuations in streamflow and peak flow responses to high melt rates, often associated with rainfall in the mountains, is important (Goodwin et al., 1997). This importance will likely increase with the projected increase in large storm events in the coming century (USDI, 2011).

There are two real-time gauging stations that are 16.2 km apart, the upstream US Geological Survey 13334450 (elevation 552 m, inflow), and the downstream Washington State Department of Ecology 35D100 (elevation 317 m, outflow) (Fig. 7b). The distributed lateral inflow is typically positive during low streamflow periods and negative at peak flows, suggesting active surface water and groundwater interactions. The lateral inflow was estimated based on water balance and the difference of hydraulic heads between stream water and a calibrated level of groundwater in the underlying aquifer following McDonald and Harbaugh (1988) and Chen and Chen (2003) and was assumed to be uniformly distributed along the channel between the two gauging stations. All the observed streamflow data are recorded in a 15-min interval and the hydrographs are shown in Fig. 8.

We assume the Asotin Creek is a trapezoidal channel. The channel configuration parameters, i.e., the bottom width and the inverse slope of the trapezoidal channel and the Manning's roughness coefficient, are calibrated using the rating curve of the gauging station WADOE35D100 with an assumption that the Q–h

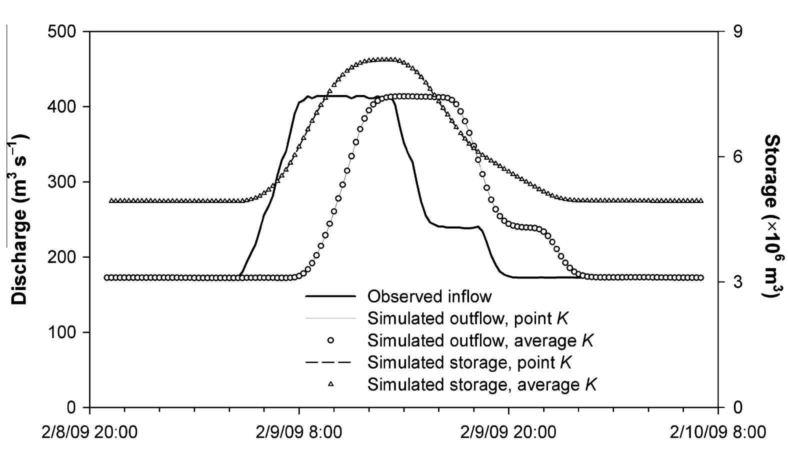

Fig. 18. Simulated outflow and channel storage using different methods for the upper reach of the Clearwater River, ID, February 8–10, 2009. Note that the simulated outflow (or storage) from the discrete Hayami solution using the point- or average kernel function values largely overlap.

relationship follows the Manning's equation. The calibrated parameters are assumed constant for the entire reach.

The simulated peak discharge is 2.0% lower than the observed value, with a root-mean-square error (RMSE) of 0.24 $m^3 s^{-1}$, when using the DHC-PKF method, and is 0.19% higher than the observed value, with a RMSE of 0.15 $m^3 s^{-1}$, when using the AKF method (Fig. 8).

Part of the simulation errors in using either the PKF or the AKF method could be due to the simplified estimation of lateral inflow. The relatively larger errors in simulating the peak discharge and total volume using the DHC-PKF method are due to the error of the integration of the discrete kernel function. For a 15-min time step, there are only 1.65 time steps for the rising limb of the kernel function (Fig. 9a) of which the integration over time is 0.987, or a −1.3% error. The solution fluctuates and becomes unreliable as the size of the time step is further increased (Fig. 9b and c). If $\Delta t \leqslant 14$ min, the number of time steps $N \geqslant 1.76$, and the integration error (ΔM) of the discrete K will be smaller than 0.62%.

A comparison of the discrete Hayami solution with the CPMC method shows that the differences between the DHC-AKF and the CPMC methods fluctuate closely to zero, with an RMSE of 0.016 $m^3 s^{-1}$, whereas the differences between the DHC-PKF and the CPMC methods tend to be substantially less than zero, though also with fluctuations, with an RMSE of 0.17 $m^3 s^{-1}$ (Fig. 10). The simulated channel water storage using the DHC-AKF is close to that by the CPMC method, while the simulated water storage using the DHC-PKF method increases unrealistically when the channel discharge continuously decreases, due to the mass balance error in calculating the outflow (Fig. 11).

This computation took a Pentium 4 PC 0.156 s when the discrete Hayami solution with either point or the average method was used, and 0.140 s when the CPMC method was used.

4.2. Clearwater River, ID

The Clearwater River is the second largest tributary to the Snake River in the Columbia Basin, US Pacific Northwest (Fig. 7a). Its middle fork has been listed as one of the nation's wild and scenic rivers in the Wild & Scenic Rivers Act passed in 1968. The recovery of salmon and steelhead habitat in Clearwater River has been an important management goal for decades (ICTRT, 2007). Adequate flow routing is crucial to understanding streamflow regime in relation to salmon migration and seasonality. There are two USGS gauging stations for the Clearwater River between Peck and Spalding, in north central Idaho State. The main tributary in this reach, the Potlatch River, joins the Clearwater River at river mile 14.9 (24 km) and is also gauged by the USGS (Table 1). Upstream of the Clearwater River near Peck is a regulated reservoir, the Dworshak Reservoir (Fig. 7c). The active operation of the reservoir generates frequent waves. For our application, we selected a single-peak wave during February 8–10, 2009 (Fig. 12) for the three reaches: the Potlatch River from the gauging station to the confluence, the Clearwater River from the upstream gauging station to the confluence with the Potlatch River, and the Clearwater River from the confluence to the downstream gauging station.

We assume the Clearwater River and the Potlatch River are trapezoidal channels. The channel configuration parameters, including the bottom width, the inverse slope, and the Manning's roughness coefficient, are calibrated using the rating curves for the USGS13341050 for the upper reach of the Clearwater River, USGS13342500 for lower reach of the Clearwater River, and USGS13341570 for the Potlatch River, with the assumption that the Q–h relationship follows the Manning's equation. The calibrated parameters are assumed constant along each reach.

4.2.1. Potlatch River, ID

For the relatively short distance (2 mi or 3.2 km) between the USGS gauging station on Potlatch River and its confluence with Clearwater River, the calculated maximum value of the discrete kernel function is 7.94E−4, at time 879 s, or 14.7 min, less than the temporal interval of 15 min for the observation data (Fig. 13a). With this temporal interval, the number of time steps on the rising limb of the kernel function is 0.7 and the integration error of the discrete kernel function using the point value is 6.6% (Fig. 13b and c). The integration error would be negligible if $\Delta t \leqslant 7$ min or $N \geqslant 1.52$, positive if $7 < \Delta t \leqslant 18$ min, and always negative if $\Delta t > 18$ min. With further increased Δt, the integration error would increase until it approached −100%, when all the effective K values were missed. The integration error of the discrete

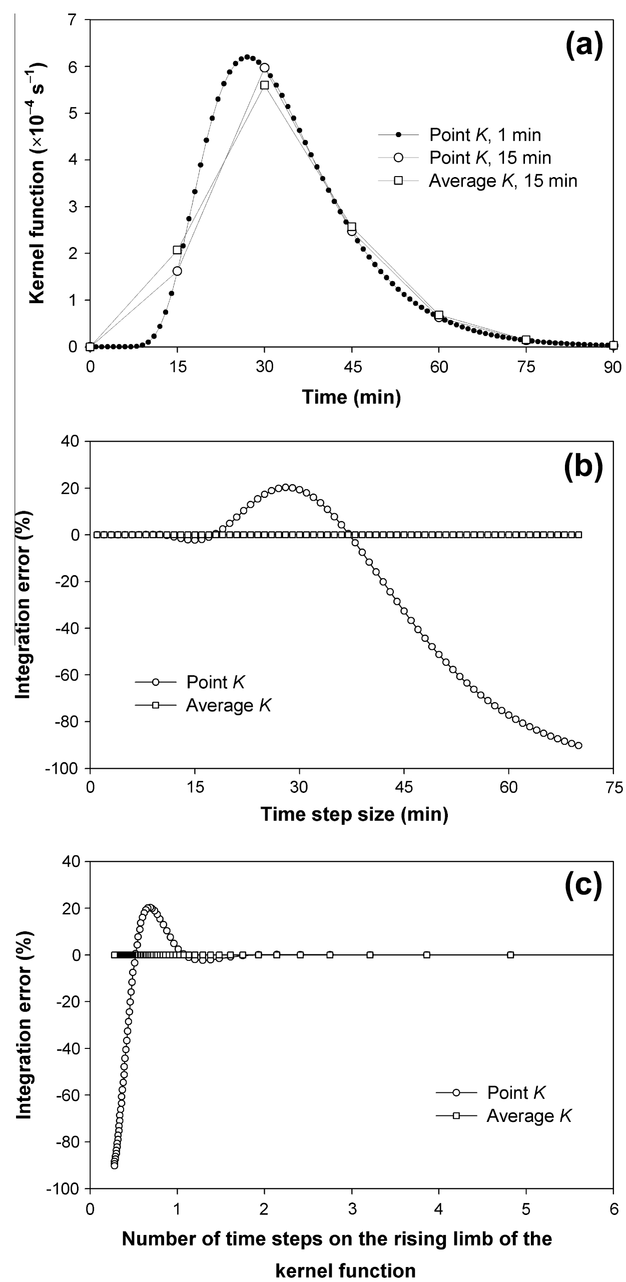

Fig. 19. Comparison of discrete Hayami kernel functions using point- or average values (a), and the effect of time step (b) and number of time steps (c) on integration errors in the discrete Hayami kernel function for channel routing, lower reach, Clearwater River, ID, February 8–10, 2009.

kernel function using the average values is negligible, regardless of the size of time step, as demonstrated in the previous case.

The simulated outflow using DHC-PKF and DHC-AKF methods and using the CPMC method are shown in Fig. 14. The result from the DHC-AKF method is very close to that from the constant-parameter Muskingum–Cunge method, and their difference is small fluctuations about zero (Fig. 15). Comparing with the CPMC method, the error of the results by the DHC-PKF method is positive when the inflow is greater than the initial condition, and negative when the inflow is less than the initial condition, and grows with time (Fig. 15).

The simulated channel storage from the DHC-AKF and from the CPMC methods are essentially identical (Fig. 16). Because of the error in the simulated discharge from the DHC-PKF method, the simulated channel storage would increase unrealistically with time even when the channel flow, and thus the channel stage, are decreasing (Figs. 14 and 16).

4.2.2. Clearwater River, ID

The upper reach of the Clearwater River flows from river mile 37.4 to 14.9 (60.2–24.0 km). With more than five steps (Δt = 15 min) on the rising limb of the Hayami kernel function, the point K values are close to the average K values (Fig. 17a) and the integration error of the discrete kernel function is negligible.

Fig. 17b and c shows that if the number of time steps on the rising limb of the kernel function $M \geqslant 1.75$ or $\Delta t \leqslant 50$ min, the integration error of the discrete kernel function using point kernel function values would be less than 0.19%. For $\Delta t \leqslant 56$ min, $N \geqslant 1.56$, and the integration error of the discrete K is less than 0.58%. For Δt ranging 57–66 min, N ranges 1.53–1.32, and the integration error of discrete K varies from −0.18% to −2.15%. For Δt ranging 67–70 min, N ranges 1.3–1.25, and the integration error of discrete K increases from 0.25% to 3.74%. The integration of the discrete K using the average K values remains unity regardless of the size of time step. The simulated outflow and channel storage by using these two methods are almost the same (Fig. 18), with a peak outflow of 413.50 $m^3 s^{-1}$ from the PKF method and 413.49 $m^3 s^{-1}$ from the AKF method. Compared with the peak inflow of 413.74 $m^3 s^{-1}$, the outflow is attenuated by both methods, with a slightly larger attenuation from the AKF method. The larger attenuation is a disadvantage of the AKF method, as a result of missing the maximum of the kernel function values due to averaging. The difference in peak attenuation from the two methods is negligible for the trapezoidal-shaped wave. It may be significant for a triangular-shaped wave.

The lower reach of the Clearwater River is from river mile 14.9, the junction with its tributary, the Potlatch River, to river mile 11.6. The inflow for this reach is the sum of the simulated outflows from the upper reach of Clearwater River and the Potlatch River. To avoid propogation of the simulation error for the Potlatch River using the PKF method, we used the simulated outflows with the AKF method as the inflow for the lower reach. For this 3.3-mi reach, there are only 1.3 time steps on the rising limb of the Hayami kernel function (Fig. 19a), with an error of −2.3% in integrating the discrete kernel function using point K values. If the number of time steps on the rising limb of the kernel function $N \geqslant 1.75$ or $\Delta t \leqslant 11$ min, the integration error of the discrete kernel function using PKF values would be less than 0.29% (Fig. 19b and c). For Δt ranging 12–17 min, N ranges 1.61–1.13, and the integration

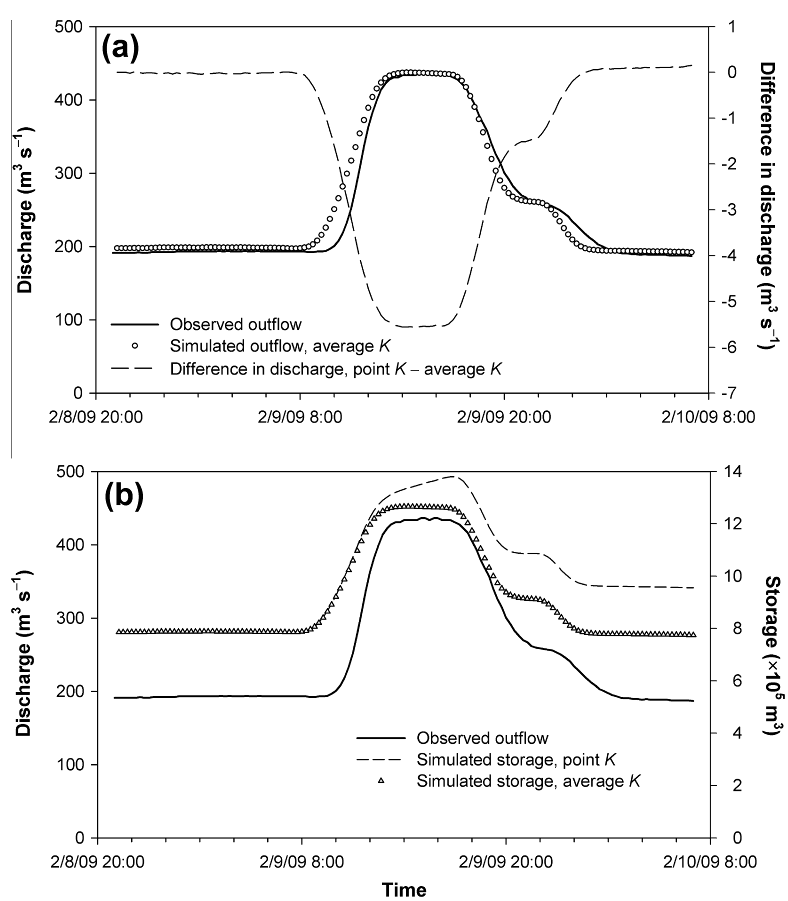

Fig. 20. (a) Comparison of observed and simulated outflow and difference in simulated outflow between point K and average K methods, and (b) observed discharge and simulated channel storage using different methods, lower reach, Clearwater River, ID, February 8–10, 2009.

error of discrete K changes from -0.88% to -2.3%. For Δt ranging 18–37 min, N ranges 1.07–0.52, and the integration error of discrete K is between 0.41% and 20%. For $\Delta t \geqslant 38$ min, $N \leqslant 0.51$, and the integration of discrete K is much less than unity. The integration error of the discrete K using the average K values is negligible regardless of the size of time step.

Though the resultant error in mass balance for the simulated outflow is small, and the simulated flow only differs during peak flow time from that by using the average K values, the effect on the simulated channel water storage is significant (Fig. 20). The differences between the simulated and the observed discharge may be caused by (i) the neglecting of the rather small amount of temporally variable lateral inflow or outflow, (ii) the use of the linear diffusion-wave model that does not account for the steepening effect of the wave, (iii) the simplification and assumptions of the channel shape and channel configuration parameters, and (iv) the assumption that the Manning equation is valid. The errors caused by (i), (iii), and (iv) can be reduced by using additional field data and a more adequate flow velocity function, and the errors from (ii) may be lowered by differentiating the non-linear system to parallel linear systems (Becker, 1976), adopting a multi-linear model (Perumal, 1994; Camacho and Lees, 1999; Perumal et al., 2007) or the modified variable-parameter Muskingum–Cunge method (Ponce and Chaganti, 1994), or dividing the channel reach into sub-reaches and applying the discrete Hayami convolution solution to each sub-reach.

5. Summary and conclusions

The Hayami convolution solution can be used in constant-parameter diffusion-wave channel routing with distributed lateral inflow. However, the convolution of channel inflow with the continuous Hayami kernel function has analytical solutions only for simplified cases and is costly when solved using numerical integration for watershed modeling that often involves hundreds of reaches. It is generally more efficient to use the discrete Hayami convolution.

The Hayami kernel function itself is continuous over time from 0 to $+\infty$, and its integration over this range is unity. Yet attention should be paid to the size of the time steps when we use its discrete exact point values in replacement of the continuous function. When the rising limb of the Hayami kernel function is shorter than 1.8 time steps in duration, the integration of the discrete Hayami kernel function using the point kernel function values is hardly unity, which would lead to mass balance error for channel routing. Hence, this solution applies only to cases with rising limb of the kernel function longer than 1.8 time steps, as demonstrated in the hypothetic numerical experiment with small time step sizes or a relatively larger time step size for a longer channel (upper reach of Clearwater River). When this criterion is not met, there is a high risk of simulated mass balance failure. This has been shown in our case applications for Asotin Creek, Potlatch River, and lower reach of Clearwater River. In Asotin Creek and lower reach of Clearwater River case applications, with 1.65 and 1.3 time steps on the rising limb of their kernel functions, respectively, the errors for simulated outflow were not too large, but the errors of the simulated water storage were significant and increased with time, as a result of the accumulation of mass balance error. In Potlatch River case application, with only 0.7 time step on the rising limb of the kernel function, the error in simulated outflow was significant and increased with time.

Another approach is to use the center-averaged kernel function values. Our hypothetic example and case applications to Asotin Creek, Potlatch River, and the upper and lower reaches of Clearwater River showed that the integration of the discrete kernel function using the averaged kernel function values is always unity, regardless of temporal resolution. Therefore, we recommend the use of this method to preserve the mass balance of channel flow when the rising limb of the kernel function is short, or in watershed channel routing with numerous channel reaches, for which the kernel functions may be different. The larger peak attenuation is a limitation of the AKF method, especially for flood forecasting. This limitation would recommend the use of the PKF method if the rising limb of the Hayami kernel function is longer than 1.8 time steps and mass balance error is minor.

Acknowledgements

This work was supported by the USDA CSREES CEAP Grant (No. 2008-48686-04903) and Washington State University. We are grateful to the two anonymous reviewers, Associate Editor, and Editor-in-Chief for their valuable comments and suggestions that have helped to improve the rigor and clarity of this manuscript.

References

Barlow, P.M., DeSimone, L.A., Moench, A.F., 2000. Aquifer response to stream-stage and recharge variations. II. Convolution method and applications. J. Hydrol. 230, 211–229.
Becker, A., 1976. Simulation of nonlinear flow systems by combining linear models. IAHS Publ. 116, 135–142.
Camacho, L.A., Lees, M.J., 1999. Multilinear discrete lag-cascade model for channel routing. J. Hydrol. 226, 30–47.
Chaudhry, M.H., 1993. Open-Channel Flow. Prentice Hall, Englewood Cliffs, NJ.
Chen, X., Chen, X.H., 2003. Stream water infiltration, bank storage, and storage zone changes due to stream-stage fluctuations. J. Hydrol. 280, 246–264.
Chow, V.T., Maidment, D.R., Mays, L.W., 1988. Applied Hydrology. McGraw-Hill, New York.
Dooge, J.C.I., 1959. A general theory of the unit hydrograph. J. Geophys. Res. 64, 241–256.
Dun, S., Wu, J.Q., Elliot, W.J., Robichaud, P.R., Flanagan, D.C., Frankenberger, J.R., Brown, R.E., Xu, A.C., 2009. Adapting the Water Erosion Prediction Project (WEPP) model for forest applications. J. Hydrol. 366, 46–54.
Fan, P., Li, J.C., 2006. Diffusive wave solutions for open channel flows with uniform and concentrated lateral inflow. Adv. Water Resour. 29, 1000–1019.
Goodwin, C.N., Hawkins, C.P., Kershner, J.L., 1997. Riparian restoration in the Western United States: overview and perspective. Restor. Ecol. 5, 4–14.
Hantush, M.M., 2005. Modeling stream–aquifer interactions with linear response functions. J. Hydrol. 311, 59–79.
Hantush, M.M., Harada, M., Marino, M.A., 2002. Hydraulics of stream flow routing with bank storage. J. Hydrol. Eng. 7, 76–89.
Hayami, S., 1951. On the propagation of flood waves. Disaster Prev. Res. Inst., Kyoto Univ., Bull. 1, 1–16.
Higdon, D., 2002. Space and space–time modeling using process convolutions. In: Anderson, C.W., Barnett, V., Chatwin, P.C., El-Shaarawi, A.H. (Eds.), Quantitative Methods for Current Environmental Issues. Springer-Verlag, London, pp. 37–56.
ICTRT (Interior Columbia Basin Technical Recovery Team), 2007. Viability Criteria for Application to Interior Columbia Basin Salmonid ESUs. Review Draft. Interior Columbia Basin Technical Recovery Team. 261 p.
Lighthill, M.J., Whitham, G.B., 1955. On kinematic waves. I. Flood movement in long rivers. Proc. R. Soc. London, Series A: Math. Phys. Sci. 229, 281–316.
Long, A.J., 2009. Hydrograph separation for karst watersheds using a two-domain rainfall-discharge model. J. Hydrol. 364, 249–256.
McDonald, M.G., Harbaugh, A.W., 1988. A modular three-dimensional finite-difference ground-water flow model. U.S. Geol. Surv., Tech. Water-Resour. Invest., Bk. 6, 586 p (Chapter A1).
McGuire, K.J., McDonnell, J.J., Weiler, M., Kendall, C., McGlynn, B.L., Welker, J.M., Siebert, J., 2005. The role of topography on catchment-scale water residence time. Water Resour. Res. 41, W05002. http://dx.doi.org/10.1029/2004WR003657.
Merkel, W.H., 2002. Muskingum-Cunge flood routing procedure in NRCS hydrologic models. In: Presented at the Second Fed. Interag. Hydrol. Model. Conf., Las Vegas, Nevada, July 28–August 1.
Moramarco, T., Pandolfo, C., Singh, V.P., 2008. Accuracy of kinematic wave and diffusion wave approximations for flood routing. I: steady analysis. J. Hydrol. Eng. 13, 1078–1088.
Moussa, R., 1996. Analytical Hayami solution for the diffusive wave flood routing problem with lateral inflow. Hydrol. Process. 10, 1209–1227.
Moussa, R., Bocquillon, C., 1996. Algorithms for solving the diffusive wave flood routing equation. Hydrol. Process. 10, 105–124.
Munier, S., Lerat, J., Belaud, G., Litrico, X., 2008. A New Compact Model Coupling Rainfall–Runoff and Routing Model to Support Reservoir Releases Management. The 13th IWRA World Water Congress 2008, Montpellier, France.
O'Connor, K.M., 1976. A discrete linear cascade model for hydrology. J. Hydrol. 29, 203–242.

Ogata, A., Banks, R.B., 1961. A Solution of the Differential Equation of Longitudinal Dispersion in Porous Media. U.S. Geological Survey Professional Paper 411-A.
Olsthoorn, T.N., 2008. Do a bit more with convolution. Ground Water 46, 13–22.
Perumal, M., 1994. Multilinear discrete cascade model for channel routing. J. Hydrol. 158, 135–150.
Perumal, M., Moramarco, T., Melone, F., 2007. A caution about the multilinear discrete lagcascade model for flood routing. J. Hydrol. 338, 308–314.
Ponce, V.M., Chaganti, P.V., 1994. Variable-parameter Muskingum-Cunge method revisited. J. Hydrol. 162, 433–439.
Singh, V.P., Wang, G.-T., Adrian, D.D., 1997. Flood routing based on diffusion wave equation using mixing cell method. Hydrol. Process. 11, 1881–1894.
Tingsanchali, T., Manandhar, S.K., 1985. Analytical diffusion model for flood routing. J. Hydraul. Eng. 111, 435–454.
Todini, E., 2007. A mass conservative and water storage consistent variable parameter Muskingum-Cunge approach. Hydrol. Earth Syst. Sci. 11, 1645–1659.
USDI (US Department of Interior), 2011. Literature Synthesis on Climate Change Implications for Water and Environmental Resources, second ed. Tech. Memo. 86-68210-2010-03. US Department of Interior Bureau of Reclamation Research and Development Office, Denver, CO. 264 p.
Wang, G.-T., Chen, S., Boll, J., Singh, V., 2003. Nonlinear convection–diffusion equation with mixing-cell method for channel flood routing. J. Hydrol. Eng. 8, 259–265.
Watson, I., Burnett, A.D., 1995. Hydrology: An Environmental Approach. CRC Press Inc., Boca Raton, pp. 457–473.